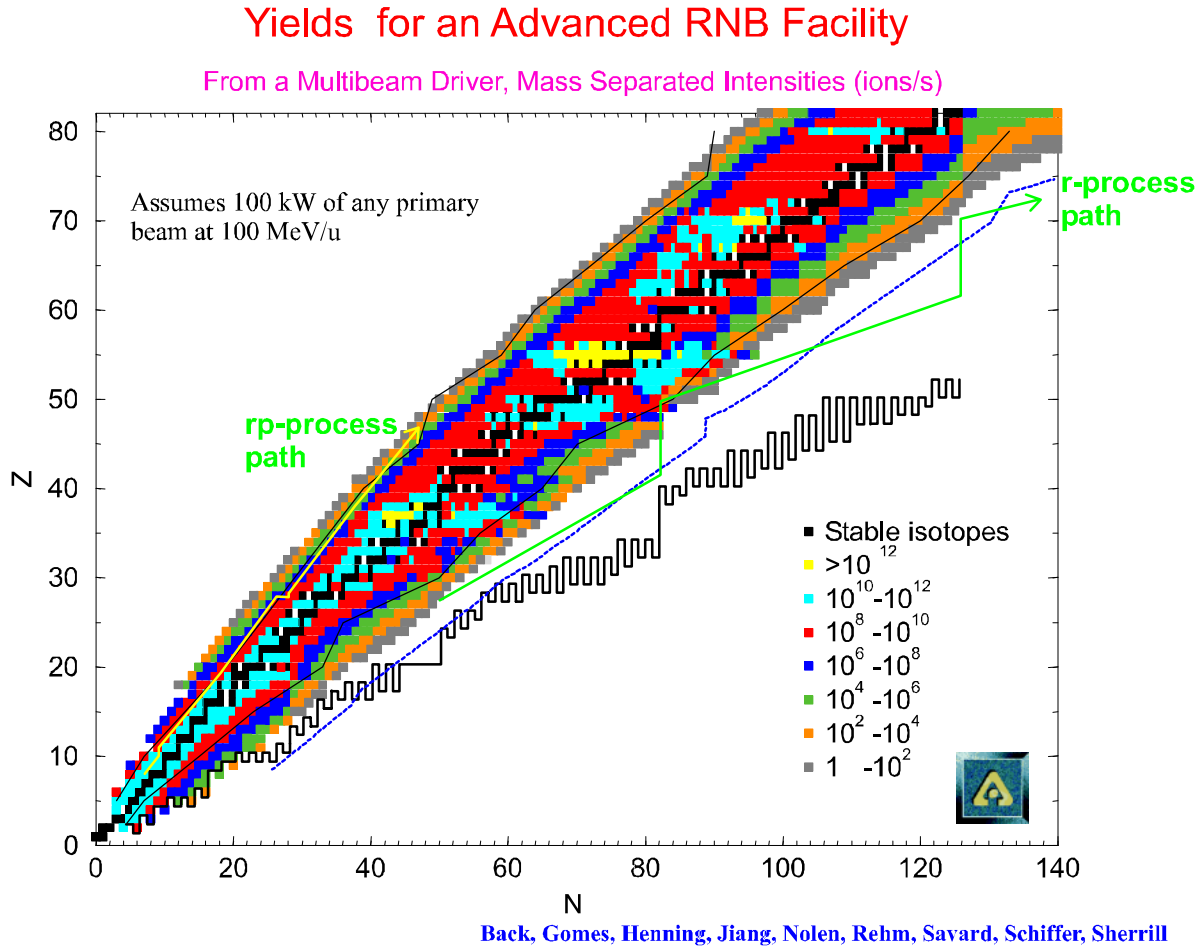


This figure is included to provide some idea of the beam intensities one might expect.



effectiveness of probing the density matrix of a loosely-bound valence particle by studying interference effects in direct reaction cross sections will depend on the magnitude of alignment of the fast exotic projectile.

Nuclear Reaction Experiments

Nuclear reactions with high-energy fragmentation beams of rare isotopes can address, among other issues, two of the key areas identified in the 1995 Long Range Plan for Nuclear Physics:

- The Phases of Nuclear Matter.
- Nuclear Astrophysics.

It is expected that intensities greater than about 10^4 particles/s will be available at RIA for $A \approx 100$ nuclei for energies up to $E/A = 400$ MeV and neutron/proton ratios ranging over about $1 < N/Z < 1.7$. This will expand the range of N/Z values for such investigations by nearly a factor of three over that studied with stable beams. Such a wide variation in the N/Z ratio will permit explorations of the isospin dependence of the liquid gas phase transition and of the nuclear equation of state. In the latter case, this information is needed to constrain extrapolations of the equation of state to the neutron-rich matter relevant to type II supernova explosions and to the stability of neutron stars.

The following section provides more information about the benefits to investigations of reaction dynamics provided by fast fragmentation beams of rare isotopes. Key issues are:

- The determination of the isospin dependence of the equation of state of nuclear matter.
- The determination of the isospin dependence of the liquid – gas phase transition of nuclear matter.
- The isospin dependence of fragment production.
- The dynamics and thermodynamics of hot nuclear systems and the development of quantum transport theory.

Nuclear Equation of State at High Density

During a central collision of two nuclei at energies of $E/A = 200 - 400$ MeV, nuclear matter densities of approaching twice the saturation density of nuclear matter can be momentarily attained. This is the only terrestrial situation in which such densities can be achieved and experimentally investigated. In Figure 34 the density dependence of the energy per nucleon is given for neutron-rich nuclear systems ($N = 2Z$) by two simple formulations (dashed and solid lines) for the isospin dependence of the nuclear equation of state (EOS) [col98]. Both formulations correspond to a soft EOS for symmetric ($N/Z = 1$; dotted line) nuclear matter with incompressibility constant $K = 200$ MeV. The extrapolation of such models towards the limit of neutron matter is an important ingredient of the theoretical modeling of the supernova explosions and the formation and stability of neutron stars. Fragmentation beams of rare isotopes at energies $E/A \approx 400$ MeV are needed to probe the isospin dependence of the EOS at densities of twice that of normal nuclear matter. Reacceleration of stopped rare isotope beams to such energies is not practical.

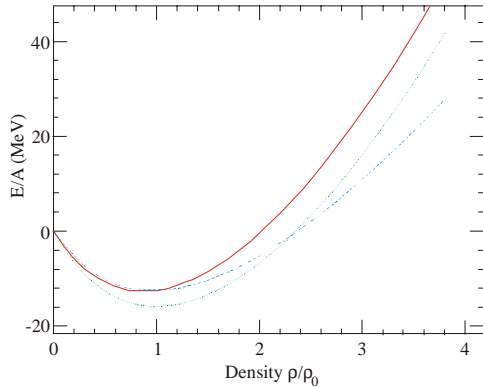


Figure 34: The nuclear equation of state, at zero temperature, for symmetric nuclear matter (dotted line) and for nuclear matter with asymmetry $(N-Z)/A = 1/3$ using the asy-soft (dashed line) and asy-stiff (solid line) isospin dependent compressibility, adapted from [col98].

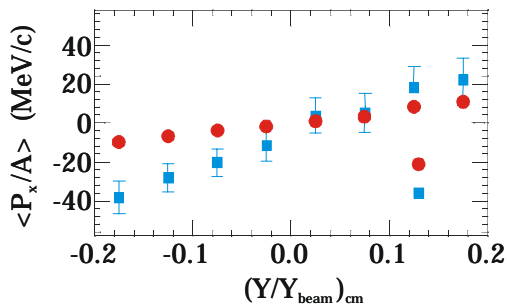


Figure 35: Average transverse momentum per nucleon for protons (solid points) and beryllium fragments (solid squares) for Kr+Au collisions at $E/A = 200$ MeV, from [hua96].

Important information about the nuclear mean field which governs the EOS can be obtained from the study of collective flow. (“Collective flow” is a set of experimental observables based on the non-thermal outward-directed component of the mean nucleonic velocity field at breakup.) In this section we discuss both experimental measurements of sideward directed flow in the reaction plane and “squeeze-out” flow perpendicular to the reaction plane.

Sidewards Directed Flow

Sideward directed flow is usually defined in terms of the ordered collective motion of nuclear matter in a reaction plane spanned by the beam velocity vector (chosen as the z direction) and the impact parameter vector (chosen as the x direction). Collective motion of particles in this plane is influenced by the Coulomb and nuclear mean field potentials and by the kinetic pressure from nucleon-nucleon collisions via the residual interaction.

The orientation of the reaction plane can be determined from the momenta of projectile or target residues or by using the transverse momentum vector method of Danielewicz and Odyniec [dan85], or by diagonalizing the transverse momentum tensor. The average transverse momentum per nucleon projected on the reaction plane, $\langle p_x/A \rangle$, is then usually determined as a function of the rapidity y^* and is usually

defined to be positive for forward emitted projectile remnants at large positive y . Values for $\langle p_x/A \rangle$ increase monotonically with y ; the slope $F = d\langle p_x/A \rangle/dy$ is the directed transverse flow F . Figure 35 shows a comparison between the transverse flow of protons and beryllium fragments for Kr + Au collisions at $E/A = 200$ MeV [hua96]. Larger flow values are observed for the beryllium fragments due to the interplay of the collective flow

* The rapidity y is defined by $y = \frac{1}{2} \frac{\ln(1 + p_{\parallel}/E)}{\ln(1 - p_{\parallel}/E)}$, where p_{\parallel} is the momentum component parallel the beam axis and E is the energy of the particle.

velocity, which contains the flow information and is independent of mass, with the random thermal velocity, which smears out the flow signal and is inversely proportional to mass.

The information that may be derived from flow depends strongly upon the incident energy. At low energies, $E/A \approx 10$ MeV, the Pauli exclusion principle blocks most nucleon-nucleon collisions and the attraction of the mean field dictates largely attractive momentum transfers to the emitted particles (i.e. predominantly negative deflection angles). At higher incident energies, $E/A \approx 200$ MeV, nucleon-nucleon collisions are not strongly blocked, leading to predominantly repulsive momentum transfers (i.e. predominantly positive deflection angles). The interplay between the attractive mean field and repulsive nucleon-nucleon collisions leads to the disappearance of sideward directed flow at a value for the incident energy termed the balance energy, E_{bal} . At higher incident energies of $E/A = 150 - 400$ MeV, well above the balance energy, nuclear matter densities of approximately twice the saturation density of nuclear matter can be momentarily attained. At such densities, collective flow observables display sensitivity to the compressibility of the nuclear equation of state.

Balance Energy

Values for the balance energy have been extracted for a variety of systems, providing tests of our present understanding of the momentum dependence of the mean field and of

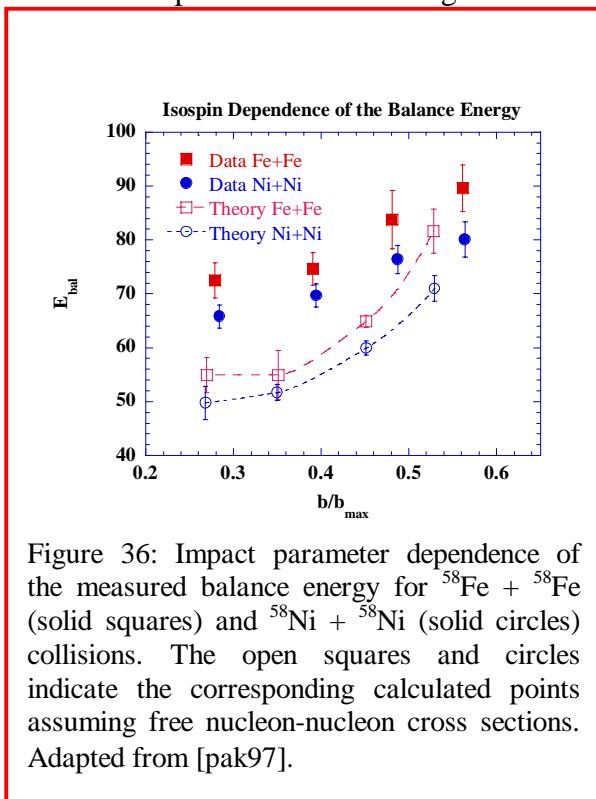


Figure 36: Impact parameter dependence of the measured balance energy for $^{58}\text{Fe} + ^{58}\text{Fe}$ (solid squares) and $^{58}\text{Ni} + ^{58}\text{Ni}$ (solid circles) collisions. The open squares and circles indicate the corresponding calculated points assuming free nucleon-nucleon cross sections. Adapted from [pak97].

the density and isospin dependencies of the in-medium nucleon-nucleon cross section. The solid circle and squares in Figure 36 shows the experimental values for E_{bal} extracted for $^{58}\text{Fe} + ^{58}\text{Fe}$ and $^{58}\text{Ni} + ^{58}\text{Ni}$ collisions, respectively [pak97]. Larger values of the balance energy are observed for the more neutron-rich $^{58}\text{Fe} + ^{58}\text{Fe}$ system than for the more symmetric $^{58}\text{Ni} + ^{58}\text{Ni}$ system.

A similar difference between values for the $^{58}\text{Fe} + ^{58}\text{Fe}$ and $^{58}\text{Ni} + ^{58}\text{Ni}$ systems is calculated using the Boltzmann-Uehling-Uhlenbeck equation (open circles and squares) and free nucleon-nucleon cross sections; this calculated difference is due to the isospin dependence of the nucleon-nucleon cross section ($\sigma_{np} \gg \sigma_{pp}, \sigma_{nn}$). (Comparatively little sensitivity to the isospin dependence of the nuclear mean field was displayed by the model calculations.) The overall magnitude of the

balance energy is underestimated. This trend suggests a reduction in the in-medium nucleon-nucleon cross sections below their values in free space. The form of the reduction of the in-medium cross sections required to reproduce the observed trends is

not presently known, however, and additional studies with systems of greater isospin asymmetry are needed to address this issue.

The availability of intense fast fragmentation beams of rare isotopes at RIA will permit more precise determinations of isospin dependencies of the in-medium modifications to the nucleon-nucleon cross sections. Beams with intensities of the order of 10^4 particles/s or greater are very suitable for such studies. For the mass 58 system, for example, one can compare $^{58}\text{Ti} + ^{58}\text{Fe}$ collisions to $^{58}\text{Zn} + ^{58}\text{Ni}$ collisions thereby extending the range of

Neutron Stars

At the end of the life of a massive star, its iron-like core collapses and the resulting supernova explosion disperses the outer part of the star into the interstellar medium. In most cases the explosion leaves behind a part of the core, an extraordinarily dense object, a neutron star with a typical mass 1.5 times that of the sun and a radius of about 10 km. Intense gravitational forces compress the star, which at its center has a density 10^{15} times that of water. As one descends from a neutron star's surface toward its center one passes through an iron-like solid crust; a region whose ratio of neutrons to protons thereby increases; into regions where nuclei may have linear or sheet-like shapes; then after about one kilometer into a region containing a nuclear fluid mostly composed of neutrons and trace amounts of protons and electrons; and finally at higher densities into a more or less unknown region near the stellar center, which may contain muons, heavy relatives of electrons, pions, kaons, lambda or sigma baryons, or even quark matter or quark-matter droplets.

It appears that large parts of a neutron star could exist in a mixed phase, for example, a mixture of ordinary hadronic matter and quark matter. The experimental and theoretical exploration of the structure of neutron-star matter and the determination of the equation of state (EOS) associated with such high-density matter is of key importance for understanding the physics of neutron stars and supernova explosions.

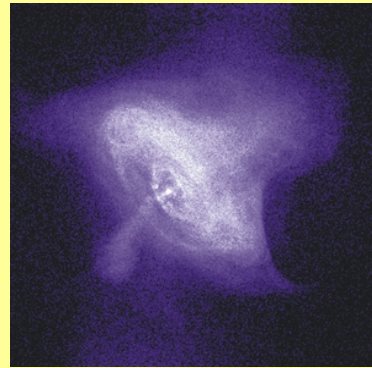


(Figure adapted from: http://chandra.harvard.edu/photo/0052/0052_xray_lg.jpg
Text from: "Opportunities in Nuclear Astrophysics: Origin of the elements", Conclusions of a Town Meeting held at the University of Notre Dame, 7-8 June 1999)

asymmetry $(N-Z)/A$, for such comparisons by 250% and providing enhanced sensitivity to isospin effects. Comparable studies can be performed in the mass 100 range (e.g. $^{106}\text{Zr} + ^{106}\text{Pd}$ and $^{106}\text{Sb} + ^{106}\text{Cd}$) and for higher mass systems as well. Isolation and quantitative understanding of the isospin dependent in-medium nucleon-nucleon cross sections at the

balance energy will enable more precise computations of such effects at higher incident energies where the isospin dependence of the EOS will be measured.

Isospin Dependence of the EOS

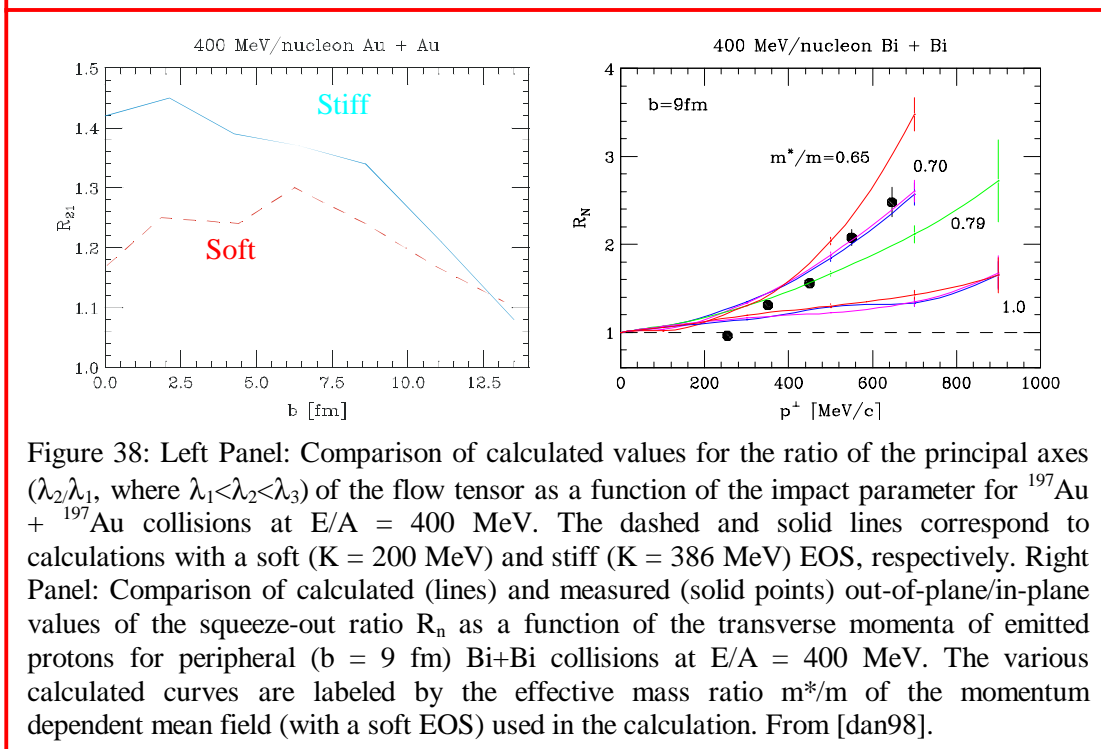
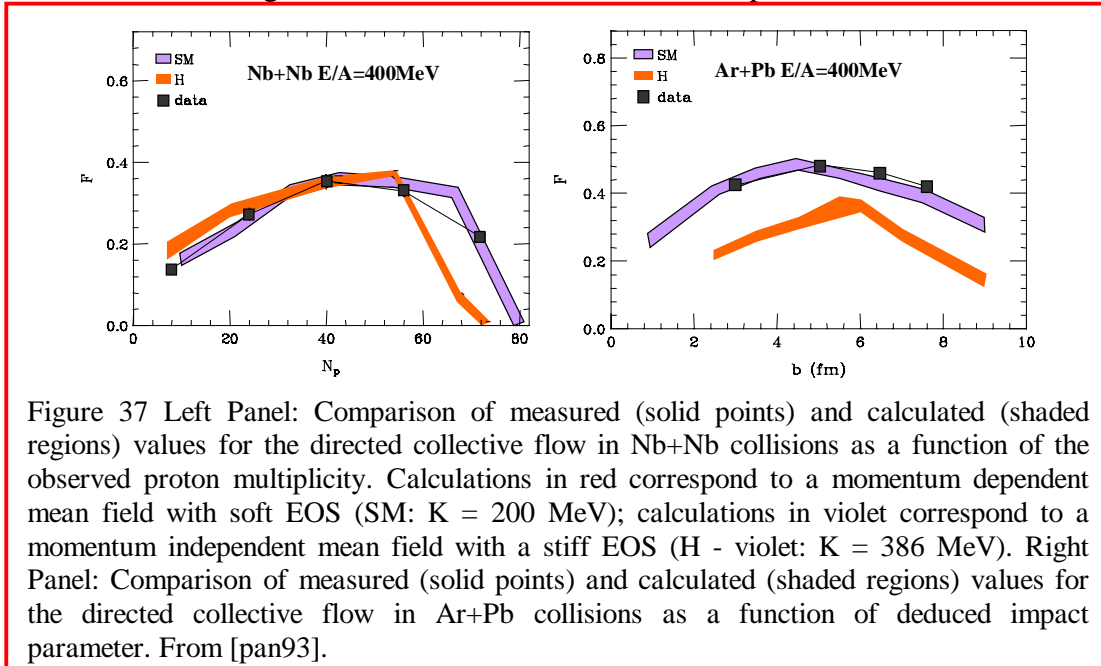
The bulk symmetry energy of nuclear matter describes the dependence of the energy on the relative number of neutron and protons. Among other things, it reflects the difference in the nuclear interaction between two neutrons or two protons, and the stronger interaction between a neutron and a proton. The symmetry energy is of great importance for studies of neutron stars, nucleosynthesis, and supernovae. It affects the collapse of massive stars, neutrino emission rates, the cooling rates of protoneutron-stars, and the predicted correlation between the radius of a neutron star and the pressure of neutron-star matter near normal nuclear densities.

Both the magnitude and the density dependence of the symmetry energy are poorly known. At present studies of the nuclear equation of state and the related compressibility of nuclear matter are limited to studies of systems with comparable neutron and proton numbers corresponding to the valley of beta stability. In dense astrophysical environments the proton to neutron ratio is closer to 0.15; densities ranging from a fraction of normal nuclear matter density to several times normal nuclear matter density are relevant. Measurements sensitive to the density dependence of the nuclear symmetry energy are particularly valuable.

The momentary attainment of high densities in central heavy ion collisions at $E/A > 200$ MeV has motivated experimental investigations of the nuclear equation of state at high density. Theoretical analyses have revealed directed transverse flow measurements and squeeze-out flow measurements to be sensitive to the compressibility of nuclear matter and to the uncertainties in the momentum dependence of the nuclear mean field and the in-medium nucleon-nucleon cross sections. The sensitivity to quantities other than the EOS results in ambiguities in the extraction of the compressibility of nuclear matter from individual flow measurements. This is illustrated in the left side of Figure 37 where similar flow values are obtained for both a momentum independent stiff EOS (H: $K = 386$ MeV) and for a momentum dependent soft EOS (SM: $K = 200$ MeV) [pan93]. This ambiguity can be broken and a preference for a soft EOS can be established if a similar analysis is performed of the asymmetric Ar+Pb system at $E/A=400$ MeV as shown in the right panel of the figure [pan93]. This illustrates the importance of measuring a broad range of systems and observables.

With fragmentation beams of rare isotopes at $E/A > 200$ MeV, the isospin dependence of the EOS can be explored by comparing symmetric systems such as $^{58}\text{Ti} + ^{58}\text{Fe}$, $^{58}\text{Zn} + ^{58}\text{Ni}$, $^{106}\text{Zr} + ^{106}\text{Pd}$, and $^{106}\text{Sb} + ^{106}\text{Cd}$ to asymmetric systems such as $^{58}\text{Ti} + ^{106}\text{Pd}$ and $^{58}\text{Zn} + ^{106}\text{Cd}$. Additional information can be obtained by investigating the squeeze-out phenomenon through comparisons of the emission out of the reaction plane to that in the reaction plane. For example, one can diagonalize the flow tensor and determine the principal axes $\lambda_1 < \lambda_2 < \lambda_3$. This is illustrated in the left panel of Figure 38, where the ratio $R_{21} = \lambda_2/\lambda_1$ of the principal axis, λ_2 , out of the reaction plane divided by the shorter of the two in-plane principal axes, λ_1 , is shown for central Au + Au collisions at $E/A = 400$ MeV. The predicted differences between calculations assuming a stiff EOS (solid line) and a soft

EOS (dashed line) display a strong sensitivity of this observable to the EOS which has, until now, not been adequately utilized. The right panel of Figure 38 shows a comparison between predicted and measured values for a similar quantity R_n , derived from the measured azimuthal distribution, as a function of the transverse momentum. These calculations predict that this observable provides a strong sensitivity to the momentum dependence of the nuclear mean field. Clearly, equipment designed to measure the isospin dependence of the nuclear EOS will be needed. As such experiments can be performed with moderately thick targets, investigations of the isospin dependence of the nuclear EOS can be undertaken using beams with intensities as low as 10^4 particles/s.



The liquid-gas phase transition in neutron-rich matter

Theoretically, there is little doubt that nuclear matter has a bulk phase transition at sub-nuclear density between a Fermi liquid, characteristic of nuclear matter at low excitation energies, and a nucleonic gas. It constitutes one of two bulk phase transitions of strongly interacting matter; the other is the transition from a hadronic gas to a plasma of quarks and gluons. Both phase transitions may be studied experimentally in the mesoscopic domain via measurements of heavy ion collisions. Finite size effects are expected to modify the properties of the nuclear liquid-gas phase transition; analogous finite size modifications have been observed for the solid-liquid phase transition in metallic clusters.

The multiple emission of intermediate mass fragments $3 \leq Z \leq 30$ is one predicted consequence of the liquid-gas phase transition of nuclear matter. Experiments have identified such multifragmentation processes in both central and peripheral heavy ion collisions. The left panel of Figure 39 shows the incident energy dependence of the

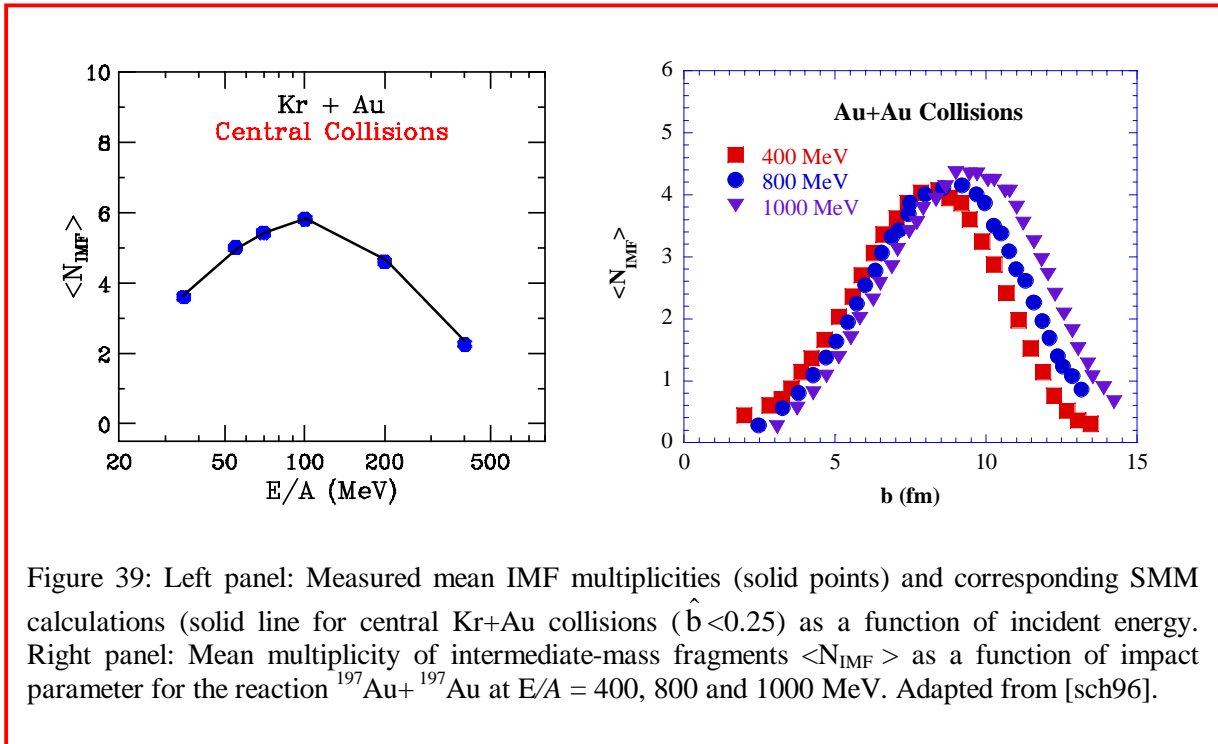


Figure 39: Left panel: Measured mean IMF multiplicities (solid points) and corresponding SMM calculations (solid line for central Kr+Au collisions ($\hat{b} < 0.25$) as a function of incident energy. Right panel: Mean multiplicity of intermediate-mass fragments $\langle N_{IMF} \rangle$ as a function of impact parameter for the reaction $^{197}\text{Au} + ^{197}\text{Au}$ at $E/A = 400, 800$ and 1000 MeV. Adapted from [sch96].

multiplicity of Intermediate Mass Fragments (IMF's) produced in central Kr + Au collisions [pea94]. Multifragmentation events are observed for incident energies in the range of $E/A = 35 - 200$ MeV. The right panel shows the impact parameter dependence for the fragmentation of Au projectiles at a variety of incident energies [sch96]. In both cases, fragment multiplicities increase to a maximum with increasing energy deposition (increasing incident energy for central collisions or decreasing impact parameter for peripheral collisions). Then the fragment multiplicity declines with energy deposition as the system begins to vaporize completely into nucleons and light particles.

Large fragment multiplicities like those in Figure 39 have been reproduced via the Expanding Evaporating Source (EES) model [fri90], or via multiparticle phase space models like the Statistical Multifragmentation Model (SMM) [bon95] or the Berlin Multifragmentation Model (BMM) [gro97] which assume that fragmentation occurs as a result of a low density phase transition similar to the liquid gas phase transition of nuclear matter. In contrast, conventional compound nuclear fission or evaporation models typically produce IMF multiplicities of the order of unity. As an example of how well the statistical multifragmentation models reproduce the experimental multifragmentation data, Figure 40 shows a comparison between the measured charge distributions for central Au+Au collisions at $E/A=35$ MeV and corresponding SMM calculations [dag96]. Similar results can also be obtained for peripheral collisions at much higher incident energies, indicating that both peripheral heavy ion collisions at $E/A=400$ MeV and mass-symmetric central heavy collisions at $E/A \approx 35-40$ MeV offer optimal conditions for investigating statistical properties such as the isospin dependence of the nuclear

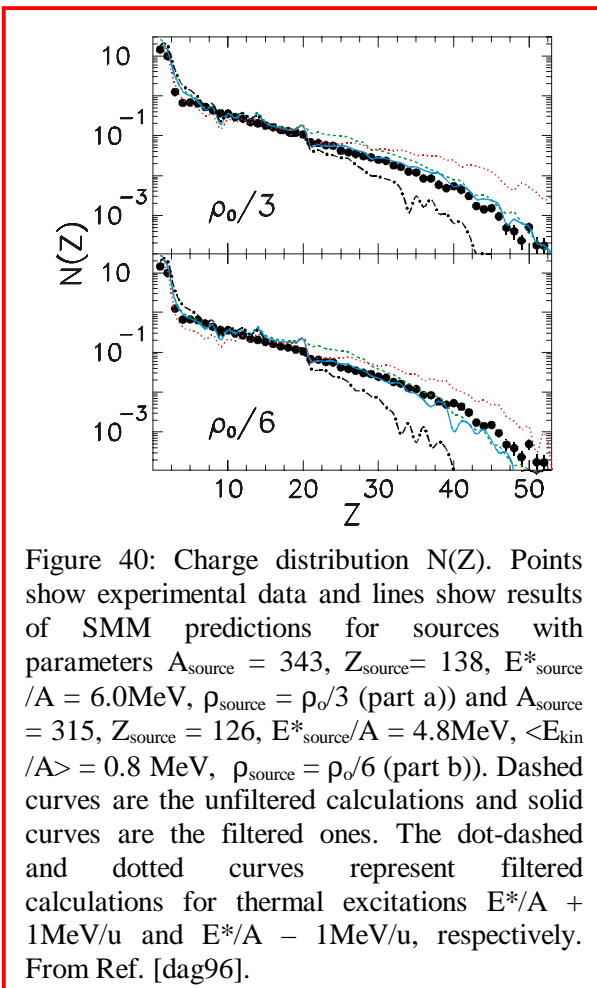


Figure 40: Charge distribution $N(Z)$. Points show experimental data and lines show results of SMM predictions for sources with parameters $A_{\text{source}} = 343$, $Z_{\text{source}} = 138$, $E_{\text{source}}^*/A = 6.0$ MeV, $\rho_{\text{source}} = \rho_0/3$ (part a)) and $A_{\text{source}} = 315$, $Z_{\text{source}} = 126$, $E_{\text{source}}^*/A = 4.8$ MeV, $\langle E_{\text{kin}}/A \rangle = 0.8$ MeV, $\rho_{\text{source}} = \rho_0/6$ (part b)). Dashed curves are the unfiltered calculations and solid curves are the filtered ones. The dot-dashed and dotted curves represent filtered calculations for thermal excitations $E^*/A + 1$ MeV/u and $E^*/A - 1$ MeV/u, respectively. From Ref. [dag96].

liquid-gas phase transition.

liquid-gas phase transition.

Isospin dependence of statistical multifragmentation

The symmetry term in the nuclear matter EOS is anticipated to be the principal origin of the isospin dependence of the nuclear liquid gas phase transition. Pure neutron matter is probably unbound and does not exist in the liquid phase. Due to the weak binding of neutron rich matter, the region of mixed phase equilibrium is expected to shrink with increasing neutron excess. Models for the liquid-gas phase transition in two-component (neutron and proton) nuclear matter also predict that the coexistence region for neutron-rich matter will display fractionation effects wherein the gas is significantly more neutron-rich than the liquid. Analogous situations are encountered in the crusts of neutron stars where very large $A \approx 1000$ “spaghetti” and “lasagna” nuclei form around the few protons that are present in the region of the inner crust.

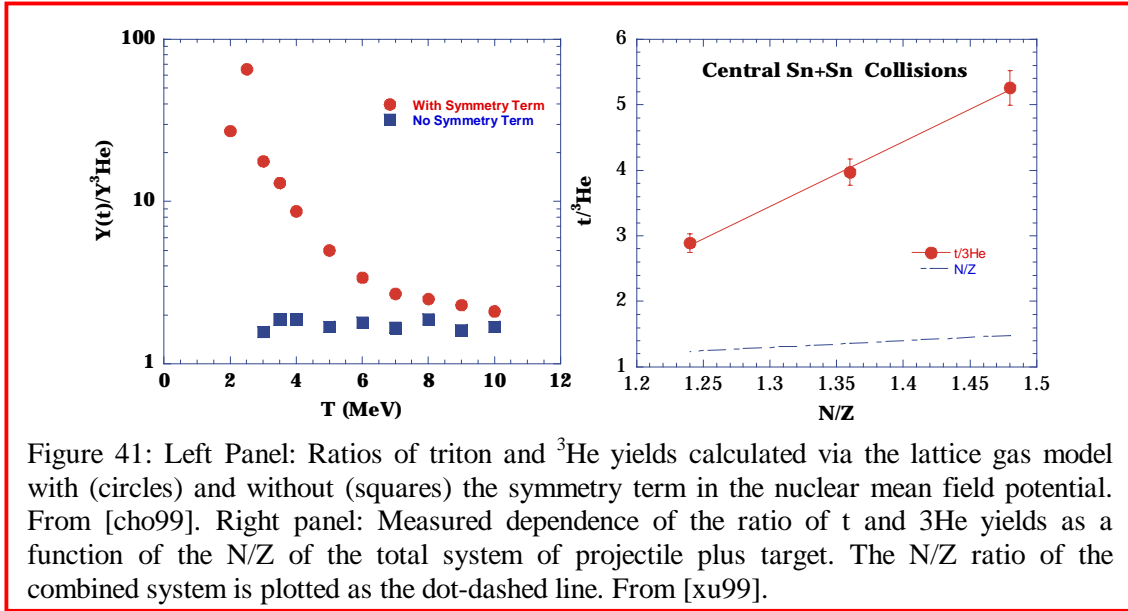
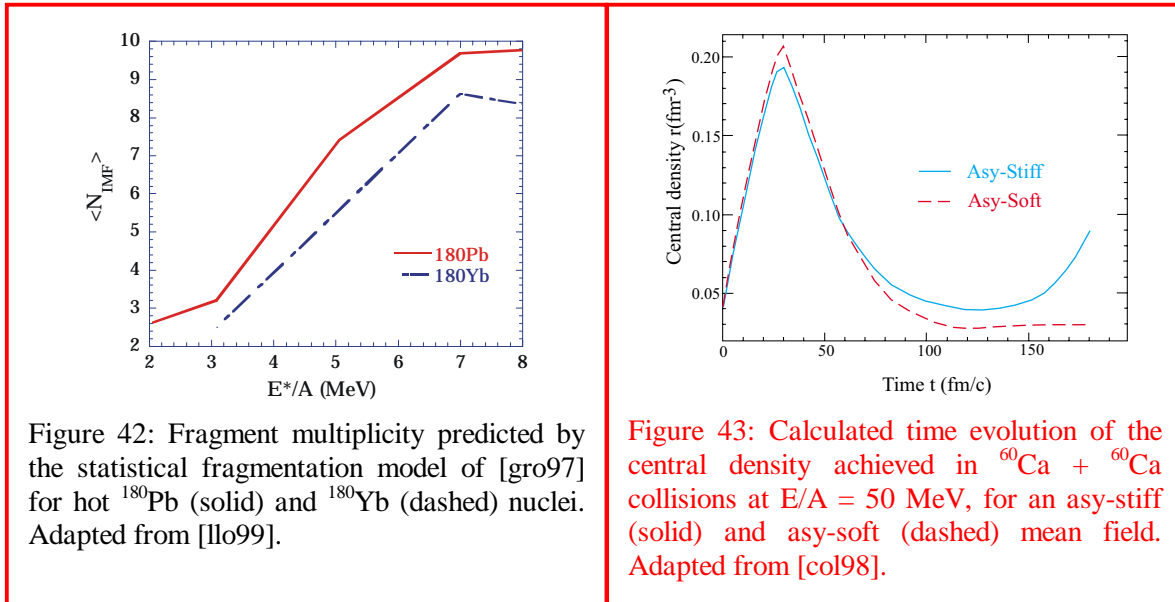


Figure 41: Left Panel: Ratios of triton and ^3He yields calculated via the lattice gas model with (circles) and without (squares) the symmetry term in the nuclear mean field potential. From [cho99]. Right panel: Measured dependence of the ratio of t and ^3He yields as a function of the N/Z of the total system of projectile plus target. The N/Z ratio of the combined system is plotted as the dot-dashed line. From [xu99].

Fast fragmentation beams of rare isotopes offer the unique opportunity to explore the isospin dependence of multifragmentation and the liquid-gas phase transition. Ideally, such experiments would be performed in inverse kinematics by fragmenting a rare isotope beam projectile. Fast fragmentation beams from RIA with energies of $E/A > 200$ MeV and intensities of 10^4 particles/s or more are ideal for this purpose. For example, one can compare the projectile multifragmentation of ^{106}Zr ($N/Z \approx 1.7$) to that of ^{106}Sb ($N/Z \approx 1.1$). The kinematics of projectile fragmentation also has the advantage of reducing the solid angle coverage needed in the laboratory frame and lowering the detection thresholds in the rest frame of the emitting source.

Expected enhancements of the isospin asymmetry of the gas can be explored via measurements of quantities like t - ^3He yield ratio, which is less influenced by secondary decay of particle unstable fragments than the n/p ratio. The left panel of Figure 41 shows the temperature dependence of the t - ^3He ratio predicted for a nuclear system undergoing a phase transition within a lattice gas model [cho99]. Calculations that neglect the symmetry term in the nuclear EOS are denoted by the square points, which deviate little from the N/Z value (≈ 1.7) of the combined system. Calculations, which model the symmetry term in the nuclear EOS, display a considerable amplification of the isospin asymmetry of the gas phase and enhanced t - ^3He ratios (circular points) which attain values in excess of 50 at $T \approx 2.4$ MeV. Experimental t - ^3He yield ratios obtained for central $^{112}\text{Sn} + ^{112}\text{Sn}$, $^{112}\text{Sn} + ^{124}\text{Sn}$ and $^{124}\text{Sn} + ^{124}\text{Sn}$ collisions [xu99], shown in the right panel of Figure 41, increase rapidly with the N/Z of the system supporting the idea that light particles (which contribute to the gas phase) are proportionately more neutron-rich than the overall system.

Besides these fractionation effects, it will be important to investigate the sensitivity of the fragment multiplicities and charge distributions to the isospin of the system. As an example, Figure 42 compares IMF multiplicities predicted by equilibrium BMM statistical calculations for the decay of hot ^{180}Pb and ^{180}Yb nuclei [llo99]. These calculations predict a shift of 1 MeV/nucleon for the threshold of multifragmentation. To make the expected



differences as large as possible, the corresponding measurements should be performed with beams that have the widest range of N/Z values possible. Energies of $E/A > 200$ MeV and intensities of 10^4 particles/s or more are ideal for these measurements. It should be possible to test these effects by comparing the fragmentation of projectiles at N/Z values over the range $1 < N/Z < 1.7$ using the fast fragmentation beams of RIA.

Isospin dependence of dynamic fragmentation and multifragmentation

While systems produced in low energy central collisions ($E/A < 50$ MeV) expand slowly and may equilibrate, multifragmentation may occur without achieving equilibrium between liquid and gaseous phases at higher incident energies. There, a spinodal decomposition of the system may occur when the density of the system approaches one third that of normal nuclear matter, becomes adiabatically unstable and density fluctuations grow exponentially.

Calculations predict that expansion and subsequent dynamical multifragmentation depend on the adiabatic incompressibility of the low density EOS for incident energies near the threshold of dynamical multifragmentation ($E/A \approx 50$ MeV). For neutron rich radioactive beams, the symmetry term in the nuclear equation of state makes an important contribution to the incompressibility and may determine whether or not dynamical multifragmentation occurs.

To illustrate the influence of the mean field upon expansion, Figure 43 show the time evolution of the central density for $^{60}\text{Ca} + ^{60}\text{Ca}$ collisions at $E/A = 50$ MeV. Results for two different formulations for the density dependence of the symmetry term are shown [col98]. For a symmetry term with a soft low density EOS (dashed line in Figures 43 and 34), the system expands to a very low density; multifragmentation in the region of adiabatic instability is likely. For a symmetry term with a stiff low density EOS (solid lines in Figures 43 and 34), the systems re-contracts and a residue is formed; multifragmentation is comparatively unlikely.

These calculations predict that measurements of fragment multiplicities as a function of the isospin of the system will help to refine dynamical multifragmentation theories and to provide constraints on the isospin dependence of the EOS at low density. Systems with very different N/Z ratios are necessary for such studies. Comparisons of $^{52}\text{Ca} + ^{48}\text{Ca}$ collisions (N/Z=1.5) to $^{50}\text{Fe} + ^{50}\text{Cr}$ collisions (N/Z=1), for example, can be performed at E/A=50 MeV with fast fragmentation beams of rare isotopes. Intensities of the order of 10^4 particles/s should be sufficient for such investigations.

References

The list of references is not intended to be a complete bibliography, but rather a guidance to reviews and the most recent papers where the individual topics are discussed in more detail.

- [abe90] S. Åberg, H. Flocard, and W. Nazarewicz, *Ann. Rev. Nucl. Part. Sci.* **40**, 439 (1990).
- [abo95] Y. Aboussir, J. M. Pearson, A. K. Dutta, and F. Tondeur, *At. Data Nucl. Data Tables* **61**, 127 (1995).
- [ann95] R. Anne *et al.*, *Z. Phys. A* **352**, 397 (1995).
- [asa90] K. Asahi *et al.*, *Phys. Lett. B* **251**, 489 (1990).
- [auf94] M. B. Aufderheide, I. Fushiki, G. M. Fuller and T. A. Weaver, *Astro. J.* **424**, 257 (1994).
- [aum99] T. Aumann *et al.*, *Nucl. Phys. A* **649**, 297c (1999).
- [aum99] T. Aumann *et al.*, *Phys. Rev. Lett.*, in press (1999).
- [aus99] S. M. Austin private communication.
- [azh98] A. Azhari *et al.*, *Phys. Rev. C* **57**, 628 (1998); M. Thoennessen *et al.*, *International School of Heavy-Ion Physics, 4th Course: Exotic Nuclei*, R. A. Broglia and P. G. Hansen (eds.), (World Scientific, Singapore, 1998), p. 269.
- [bau93] E. Bauge *et al.*, *Phys. Rev. Lett.*, **70**, 3705 (1993).
- [ber83] A. M. Bernstein, V. R. Brown, V. A. Madsen, *Comm. Nucl. Part. Phys.* **11**, 203 (1983).
- [ber88] C. A. Bertulani and G. Baur, *Phys. Rep.* **163**, 299 (1988).
- [ber99] C. A. Bertulani, *Comp. Phys. Comm.* **116**, 345 (1999).
- [bla80] J. P. Blaizot, *Phys. Rep.* **64**, 171 (1980).
- [bon95] J. P. Bondorf *et al.*, *Phys. Rep.* **257**, 133 (1995).
- [bon98] A. Bonaccorso and D. M. Brink, *Phys. Rev. C* **58**, 2864 (1998).
- [bor93] M. J. G. Borge *et al.*, *Nucl. Phys. A* **560**, 664 (1993).
- [bra99] "Proceedings of the Topical Conference on Giant Resonances", edited by A. Bracco and P. F. Bortignon, *Nucl. Phys. A* **649** (1999).
- [bro88] B. A. Brown and B. H. Wildenthal, *Ann. Rev. Nucl. Sci.* **38**, 191 (1988).
- [bro96] B. A. Brown and P. G. Hansen, *Phys. Lett. B* **381**, 391 (1996).
- [bue84] M. Buenerd, *J. Phys. (Paris), Colloq.* **C-4**, 115 (1984).
- [che95] B. Chen *et al.*, *Phys. Lett. B* **355**, 37 (1995).
- [chi93] A. A. Chishti *et al.*, *Phys. Rev. C* **48**, 2607 (1993).

- [cho95] W.-T. Chou *et al.*, Phys. Rev. C **51**, 2444 (1995).
[cho99] Ph. Chomaz and F. Gulminelli, Phys. Lett. B **447**, 221 (1999).
[chr97] M. J. Chromik *et al.*, Phys. Rev. C **55**, 1676 (1997).
[col98] M. Colonna, M. DiToro, G. Fabbri, and S. Maccarone, Phys. Rev. C **57**, 1410 (1998).
[dag96] M. D'Agostino *et al.*, Physics Letters B **371**, 175 (1996).
[dan85] P. Danielewicz and G. Odyniec, Phys. Lett. B **175**, 146 (1985).
[dan98] P. Danielewicz, nucl-th 9907098.
[dav96] C. N. Davids *et al.*, Phys. Rev. Lett. **76**, 592 (1996).
[dav98] C. N. Davids *et al.*, Phys. Rev. Lett. **80**, 1849 (1998).
[dob94] J. Dobaczewski *et al.*, Phys. Rev. Lett. **72**, 981 (1994).
[dob96] J. Dobaczewski *et al.*, Phys. Rev. C **53**, 2809 (1996).
[dob96] J. Dobaczewski, W. Nazarewicz, and T. Werner, Phys. Scripta **T56**, 15 (1996).
[efi70] V. M. Efimov, Sov. J. Nucl. Phys. **12**, 589 (1970); Comments Nucl. Part. Phys. **19**, 271 (1990).
[end90] P. M. Endt *et al.*, Nucl. Phys. A **521**, 1 (1990).
[far97] Michel Farine *et al.*, Nucl. Phys. **A615**, 135 (1997), T. v. Chossy and W. Stocker, Phys. Rev. C **56**, 2518 (1997), I. Hamamoto, H. Sagawa, and X. Z. Zhang, Phys. Rev. C **56**, 3121 (1997), D. Vretenar *et al.*, Nucl. Phys. **A621**, 853 (1997), Z. Ma *et al.*, Phys. Rev. C **55**, 2385 (1997).
[fau96] M. Fauerbach *et al.*, Phys. Rev. C **53**, 647 (1996).
[fau97] M. Fauerbach *et al.*, Phys. Rev. Rev. C **56**, R1 (1997).
[for99] S. Fortier *et al.*, Physics Letters B **461**, 22 (1999).
[foy98] B. D. Foy *et al.*, Phys. Rev. C **58**, 749 (1998).
[fri90] William A. Friedman, Phys. Rev. C **42**, 667 (1990).
[fri99] C. Freiburghaus, S. Rosswog and F.-K. Thielemann, Astro. P. Journ. **525**, L121 (1999).
[gar98] E. Garrido, D. V. Fedorov and A. S. Jensen, Phys. Rev. C **58**, R2654 (1998).
[gla97] T. Glasmacher *et al.*, Phys. Lett. B **395**, 163 (1997).
[gla98] T. Glasmacher, Ann. Rev. Nucl. Part. Sci. **48**,1 (1998).
[gol60] V. I. Goldanskii *et al.*, Nucl. Phys. **19**, 482 (1960).
[goo80] C. D. Goodman *et al.*, Phy. Rev. Lett. **44**, 1755 (1980).
[gor95] J. Görres *et al.*, Phys. Rev. C **51**, 392 (1995)
[gor98] S. Goriely, Phys. Lett. B **436**, 10 (1998).
[gro97] D. H. E. Gross, Phys. Rep. **279**, 119 (1997).
[gui90] D. Guillemaud-Mueller *et al.*, Phys. Rev. C **41**, 937 (1990).
[hab97] D. Habs *et al.*, Prog. Part. Nucl. Phys. **38**, 111 (1997).
[han95] P. G. Hansen, A. S. Jensen and B. Jonson, Ann. Rev. Nucl. Part. Sci. **45**, 591 (1995).
[hax97] W. C. Haxton, K. Langanke, Y.-Z. Qian, P. Vogel, Phys. Rev. Lett. **78**, 2694 (1997); Y.-Z. Qian, P. Vogel, and G. J. Wasserburg, Astro. Journ **513**, 956 (1999).
[hua96] M. J. Huang *et al.*, Phys. Rev. Lett. **77**, 3739 (1996).
[ibb98] R.W. Ibbotson *et al.*, Phys. Rev. Lett. **80**, 2081 (1998).

- [ibb99] R. W. Ibbotson *et al.*, Phys. Rev. C **59**,642 (1999).
[izu96] H. Izuma *et al.*, Phys. Lett. B **366**, 51 (1996).
[jew99] J. K. Jewell *et al.*, Phys. Lett. B **454**, 181 (1999).
[joh73] R. C. Johnson *et al.*, Nucl. Phys. **A208**, 221 (1973).
[kel97] J. H. Kelley *et al.*, Phys. Rev. C **56**, R1206 (1997).
[kra86] K.-L. Kratz *et al.*, Z. Phys. A **325**, 489 (1986).
[kra94] G. Kraus *et al.*, Phys. Rev. Lett. **73**, 1773 (1994).
[kud96] Y. Kudryavtsev *et al.*, Nucl. Instrum. Methods Phys. Res. B **114**, 350 (1996).
[lal99] G. A. Lalazissis, S. Raman, and P. Ring, At. Data Nucl. Data Tables **71**, 1 (1999).
[lee97] I. Y. Lee, Prog. Part. Nucl. Phys. **38**, 65 (1997).
[lin95] M. Lindroos *et al.*, Nucl. Instrum. Methods Phys. Res. A **361**, 53 (1995).
[llo99] W. Llope, Private Communication
[lon98] C. Longour *et al.*, Phys. Rev. Lett. **81**, 3337 (1998).
[mad99] V. Maddalena *et al.*, to be published.
[mar99] F. Maréchal *et al.*, Phys. Rev. C **60** 034615 (1999).
[mat96] K. Matsuta *et al.*, Hyperfine Int. **97/98**, 519 (1996).
[mis93] V. Mishin *et al.*, Nucl. Instrum. Meth. Phys. Res. B **73**, 550 (1993).
[mit97] W. Mittig, *et al.*, Annu. Rev. Nucl. Part. Sci. **47**, 27 (1997).
[moe95] P. Moeller, J. R. Nix, W. D. Meyers, and W. J. Swiatecki, At. Data Nucl. Data Tables **59**, 185 (1995).
[mot95] T. Motobayashi *et al.*, Phys. Lett. B **346**, 9 (1995).
[nak97] T. Nakamura *et al.*, Phys. Lett. B **394**, 11 (1997).
[nav98] A. Navin *et al.*, Phys. Rev. Lett. **81**, 5089 (1999).
[ney97] G. Neyens *et al.*, Phys. Lett. B **393**, 36 (1997).
[ney99] G. Neyens *et al.*, Phys. Rev. Lett. **82**, 497 (1999).
[oga99] H. Ogawa *et al.*, J. Phys. G **24**, 1399 (1999).
[orr91] N. A. Orr, *et al.*, Phys. Lett. B **258**, 29 (1991).
[pan93] Q. Pan and P. Danielewicz, Phys. Rev. Lett. **70**, 2062 (1993).
[pak97] R. Pak *et al.*, Phys. Rev. Lett. **78**, 1022 (1997).
[pea94] G. F. Peaslee *et al.*, Phys. Rev. C **49**, R2271 (1994).
[pea96] J. M. Pearson, R. C. Nayak, and S. Goriely, Phys. Lett. B **387**, 455 (1996).
[pfa96] R. Pfaff, *et al.*, Phys. Rev. C **53**, 647 (1996).
[pfe97] B. Pfeiffer *et al.*, Z. Phys. A **357**, 253 (1997).
[ril99] L. A. Riley *et al.*, Phys. Rev. Lett. **82**, 4196 (1999).
[rog87] W. F. Rogers *et al.*, Nucl. Instrum. Methods Phys. Res. A **253**, 256 (1987).
[sag98] H. Sagawa, I. Hamamoto, and X. Z. Zhang, J. Phys. G **24**, 1445 (1998).
[sch96] A. Schuttauf *et al.*, Nucl. Phys. **A607**, 457 (1996).
[sch96] H. Scheit *et al.*, Phys. Rev. Lett. **77**, 3967 (1996).
[sch98] H. Schatz *et al.*, Phys. Rep. **294**, 167 (1998).
[sch99] H. Scheit *et al.*, Nucl. Instr. Meth. A **422**, 124 (1999).
[sel92] P. J. Sellin *et al.*, Nucl. Instrum. Methods Phys. Res. A **311**, 217 (1992).
[sew97] D. Seweryniak *et al.*, Phys. Rev. C **55**, R2137 (1997).
[sim99] H. Simon *et al.*, Phys. Rev. Lett. **83**, 496 (1999).

- [sor93] O. Sorlin *et al.*, Phys. Rev. C **47**, 2941 (1993).
- [sum97] K. Summerer *et al.*, Nucl. Phys. A **616**, 341c (1997); Z. Janas *et al.*, Phys. Rev. Lett. **82**, 295 (1999).
- [thi75] C. Thibault *et al.*, Phys. Rev. C **12**, 644 (1975).
- [tho99] M. Thoennessen *et al.*, Phys. Rev. C **59**, 111 (1999); M. Chartier *et al.*, to be published; L. Chen *et al.*, to be published.
- [tho00] M. Thoennessen *et al.*, to be published.
- [tos99] J. A. Tostevin, J. Phys. G **25**, 735 (1999).
- [var99] R. L. Varner *et al.*, Proceedings of the International Workshop on Collective Excitations in Fermi and Bose Systems, edited by C. Bertulani, World Scientific (1999), p.264.
- [wan97] S. Wan *et al.*, Z. Phys. A **358**, 213 (1997).
- [wer94] T. Werner *et al.*, Phys. Lett. B **335**, 259 (1994).
- [wer96] T. Werner *et al.*, Nucl. Phys. A **597**, 327 (1996).
- [win79] A. Winther and K. Alder, Nucl. Phys. A **319**, 518 (1979).
- [win93] J. A. Winger *et al.*, Phys. Lett. B **299**, 214 (1993).
- [woo97] P. J. Woods and C. N. Davids, Ann. Rev. Nucl. Part. Sci. **47**, 541 (1997).
- [xu99] H. Xu *et al.*, Private Communication.
- [you96] D. H. Youngblood, H. L. Clark, and Y.-W. Lui, Phys. Rev. Lett. **76**, 1429 (1996).
- [you97] D. H. Youngblood, H. L. Clark, and Y.-W. Lui, Phys. Rev. C **55**, 2811 (1997).
- [you99] D. H. Youngblood, H. L. Clark, and Y.-W. Lui, Phys. Rev. Lett. **82**, 691 (1999).
- [zhu93] M. V. Zhukov *et al.*, Phys. Rep. **231**, 151 (1993).